CHAPTER 4.

1-Year (2014), 3-Year (2012—2014), and 5-Year (2010—2014) Maps of Drought and Moisture Surplus for the Conterminous United States

Frank H. Koch
John W. Coulston

INTRODUCTION

Droughts occur in most forest ecosystems of the United States, but their frequency and intensity vary widely (Hanson and Weltzin 2000). Annual seasonal droughts are typical in Western U.S. forests. In contrast, Eastern U.S. forests usually exhibit one of two predominant drought patterns: random (i.e., occurring at any time of year) occasional droughts, as typically seen in the Appalachian Mountains and the Northeast, or frequent late-summer droughts, as observed in the Southeastern Coastal Plain and the eastern side of the Great Plains (Hanson and Weltzin 2000).

In forests, diminished moisture availability during droughts, especially since they are regularly accompanied by high temperatures, can lead to substantial tree stress (Anderegg and others 2013, Peters and others 2015, Williams and others 2013). Initially, trees, like other plants, respond to this stress by decreasing fundamental growth processes such as cell division and enlargement. Photosynthesis, which is less sensitive than these fundamental processes, decreases slowly at low levels of drought stress but decreases more sharply as drought stress becomes moderate to severe (Kareiva and others 1993, Mattson and Haack 1987). In addition to these direct effects, drought stress often makes forests susceptible to attack by tree-damaging insects and diseases (Clinton and others 1993, Mattson and Haack 1987, Raffa and others 2008). Furthermore, drought increases wildland fire risk by inhibiting organic matter decomposition and lowering the moisture content of downed woody debris and other potential fire fuels (Clark 1989, Keetch and Byram 1968, Schoennagel and others 2004, Trouet and others 2010).

Forests are generally resistant to short-term droughts (Archaux and Wolters 2006), although individual tree species differ in their levels of resistance. Regardless, because of this resistance, the duration of a drought event may be more important than its intensity (Archaux and Wolters 2006). For instance, multiple consecutive years of drought (2–5 years) in a forested area are much more likely to cause high tree mortality than one very dry year (Guarín and Taylor 2005, Millar and others 2007). Therefore, a comprehensive evaluation of drought impact in forests should include analysis of moisture conditions over multiyear time windows.

In the 2010 FHM national report, we presented a methodology for mapping drought conditions across the conterminous United States (Koch and others 2013b). Our goal was to generate drought-related spatial data sets that are finer in scale than similar products available from sources such as the National Climatic Data Center (2015b) or the U.S. Drought Monitor Program (Svoboda and others 2002). The principal inputs are gridded climate data (i.e., monthly raster maps of precipitation and temperature over a 100-year period) created with the Parameter-elevation Regression on Independent Slopes (PRISM) climate mapping system (Daly and others 2002). The methodology employs a standardized indexing

approach that facilitates comparison of a given location's moisture status during different time windows, regardless of their length. The index is easier to calculate than the commonly used Palmer Drought Severity Index, or PDSI (Palmer 1965), and sidesteps some criticisms of the PDSI (summarized by Alley 1984) regarding its underlying assumptions and limited comparability across space and time. In this chapter, we applied the methodology to the most currently available climate data (i.e., the monthly PRISM data through 2014), thereby providing a sixth time step in an ongoing annual record of drought status in the conterminous United States from 2009 forward (Koch and Coulston 2015; Koch and others 2013a, 2013b, 2014, 2015).

For the first time in this series, we also mapped the degree of moisture surplus during multiple time windows. Recently, much refereed literature (e.g., Adams and others 2009, Allen and others 2010, Martínez-Vilalta and others 2012, Peng and others 2011, Williams and others 2013) has focused on reports of widespread, regional-scale forest decline and mortality due to persistent drought conditions, especially in conjunction with periods of extremely high temperatures (i.e., heat waves). However, surplus moisture availability can also be detrimental to forests. Abnormally high moisture can be a short-term stressor (e.g., an extreme rainfall event with subsequent flooding) or a long-term stressor (e.g., persistent wetness driven by a macroscale climatic pattern such as the El Niño-Southern Oscillation), either of which may contribute to tree dieback and mortality (Rozas and García-González 2012, Rozas and Sampedro 2013). Such impacts have been observed in both tropical and temperate forests (Laurance and others 2009, Rozas and García-González 2012). Although surplus-induced impacts in forests are probably not as common as drought-induced impacts, it seems sensible to develop a single index that depicts both moisture surplus and deficit conditions, thereby providing a fuller accounting of potential forest health issues.

METHODS

We acquired grids for monthly precipitation and monthly mean temperature for the conterminous United States from the PRISM Climate Group Web site (PRISM Climate Group 2015). At the time of these analyses, gridded data sets were available for all years from 1895 to 2014. However, the grids for November and December 2014 were only provisional versions (i.e., finalized grids had not yet been released for these months). For analytical purposes, we treated these provisional grids as if they were the final versions. The spatial resolution of the grids was approximately 4 km (cell area = 16 km^2). For future applications and to ensure better compatibility with other spatial data sets, all output grids were resampled to a spatial resolution of approximately 2 km (cell area = 4 km^2) using a nearest neighbor approach. The nearest neighbor approach is a computationally simple resampling method that avoids the smoothing of data values observed with methods such as bilinear interpolation or cubic convolution.

Potential Evapotranspiration Maps

As in our previous drought mapping efforts (Koch and Coulston 2015; Koch and others 2012a, 2012b, 2013a, 2013b, 2014, 2015), we adopted an approach in which a moisture index value is calculated for each location of interest (i.e., each grid cell in a map of the conterminous United States) during a given time period. Moisture indices are intended to reflect the amount of available water in a location (e.g., to support plant growth). In our case, the index is calculated based on how much precipitation falls on a location during the period of interest as well as the level of potential evapotranspiration during this period. Potential evapotranspiration measures the loss of soil moisture through plant uptake and transpiration (Akin 1991). It does not measure actual moisture loss but rather the loss that would occur if there was no possible shortage of moisture for plants to transpire (Akin 1991, Thornthwaite 1948). By including potential evapotranspiration along with precipitation, the index accounts for this expected moisture loss and thus presents a more complete picture of a location's water supply than precipitation alone.

To complement the available PRISM monthly precipitation grids, we computed corresponding monthly potential evapotranspiration (*PET*) grids using Thornthwaite's formula (Akin 1991, Thornthwaite 1948):

$$PET_m = 1.6 L_{lm} \left(10 \frac{T_m}{I}\right)^a \qquad (1)$$

where

PET_m = the potential evapotranspiration for a given month m in cm

L_{lm} = a correction factor for the mean possible duration of sunlight during month m for all locations (i.e., grid cells) at a particular latitude l [see table V in Thornthwaite (1948) for a list of L correction factors by month and latitude]

T_m = the mean temperature for month m in degrees C

I = an annual heat index, calculated as

$$I = \sum_{m=1}^{12} \left(\frac{T_m}{5}\right)^{1.514}$$

where

T_m = the mean temperature for each month m of the year

a = an exponent calculated as $a = 6.75 \times 10^{-7} I^3 - 7.71 \times 10^{-5} I^2 + 1.792 \times 10^{-2} I + 0.49239$ [see appendix I in Thornthwaite (1948) regarding calculation of I and the empirical derivation of a]

Although only a simple approximation, a key advantage of Thornthwaite's formula is that it has modest input data requirements (i.e., mean temperature values) compared to more sophisticated methods of estimating *PET* such as the Penman-Monteith equation (Monteith 1965), which requires less readily available data on factors such as humidity, radiation, and wind speed. To implement equation 1 spatially, we

created a grid of latitude values for determining the L adjustment for any given grid cell (and any given month) in the conterminous United States. We extracted the T_m values for the grid cells from the corresponding PRISM mean monthly temperature grids.

Moisture Index Maps

To estimate baseline conditions, we used the precipitation (P) and PET grids to generate moisture index grids for the past 100 years (i.e., 1915–2014) for the conterminous United States. We used a moisture index described by Willmott and Feddema (1992), which has been applied in a variety of contexts, including global vegetation modeling (Potter and Klooster 1999) and climate change analysis (Grundstein 2009). Willmott and Feddema (1992) devised the index as a refinement of one described earlier by Thornthwaite (1948) and Thornthwaite and Mather (1955). Their revised index, MI', has the following form:

$$MI' = \begin{cases} P/PET - 1 & , \quad P < PET \\ 1 - PET/P & , \quad P \geq PET \\ 0 & , \quad P = PET = 0 \end{cases} \qquad (2)$$

where

P = precipitation

PET = potential evapotranspiration

(P and PET must be in equivalent measurement units, e.g., mm)

This set of equations yields a symmetric, dimensionless index scaled between -1 and 1. MI' can be calculated for any time period, but is commonly calculated on an annual basis using summed P and PET values (Willmott and Feddema 1992). An alternative to this summation approach is to calculate MI' from monthly precipitation and potential evapotranspiration values and then, for a given time window of interest, calculate its moisture index as the mean of the MI' values for all months in the time window. This "mean-of-months" approach limits the ability of short-term peaks in either precipitation or potential evapotranspiration to negate corresponding short-term deficits, as would happen under a summation approach.

For each year in our study period (i.e., 1915–2014), we used the mean-of-months approach to calculate moisture index grids for three different time windows: 1 year (MI_1'), 3 years (MI_3'), and 5 years (MI_5'). Briefly, the MI_1' grids are the mean (i.e., the mean value for each grid cell) of the 12 monthly MI' grids for each year in the study period, the MI_3' grids are the mean of the 36 monthly grids from January 2 years prior through December of the target year, and the MI_5' grids are the mean of the 60 consecutive monthly MI' grids from January 4 years prior to December of the target year. Thus, the MI_1' grid for the year 2014 is the mean of the monthly MI' grids from January to December 2014, whereas the MI_3' grid is the mean of the grids from January 2012 to December 2014 and the MI_5' grid is the mean of the grids from January 2010 to December 2014.

Annual and Multiyear Drought Maps

To determine degree of departure from typical moisture conditions, we first created a normal grid, $MI_{i\,norm}'$, for each of our three time windows, representing the mean (i.e., the mean value for each grid cell) of the 100 corresponding moisture index grids (i.e., the MI_1', MI_3', or MI_5' grids, depending on the window; see fig. 4.1). We also created a standard deviation grid, $MI_{i\,SD}'$, for each time window, calculated from the window's 100 individual moisture index grids as well as its $MI_{i\,norm}'$ grid. We subsequently calculated moisture difference *z*-scores, MDZ_{ij}, for each time window using these derived data sets:

$$MDZ_{ij} = \frac{MI_i' - MI_{i\,norm}'}{MI_{i\,SD}'} \qquad (3)$$

where

i = the analytical time window (i.e., 1, 3, or 5 years) and

j = a particular target year in our 100-year study period (i.e., 1915–2014).

MDZ scores serve as a single numerical index that may be classified in terms of degree of moisture deficit or moisture surplus (table 4.1). The classification scheme includes categories (e.g., severe drought, extreme drought) like those associated with the PDSI. The scheme has also been adopted for other drought indices such as the Standardized Precipitation Index, or SPI (McKee and others 1993). Moreover, the breakpoints between *MDZ* categories resemble those used for the SPI, such that we expect the *MDZ* categories to have theoretical frequencies of occurrence that are similar to their SPI counterparts (e.g., approximately 2.3 percent of the time for extreme drought; see McKee and others 1993, Steinemann 2003). More importantly, because of the standardization in equation 3, the breakpoints between categories remain the same regardless of the size of the time window of interest. For comparative analysis, we generated and classified *MDZ* maps of the conterminous United States, based on all three time windows, for the target year 2014.

RESULTS AND DISCUSSION

The 100-year (1915–2014) mean annual moisture index, or $MI_{1\,norm}'$, grid (fig. 4.1) provides an overview of climatic regimes in the conterminous United States. (The 100-year $MI_{3\,norm}'$ and $MI_{5\,norm}'$ grids were very similar to the mean $MI_{1\,norm}'$ grid, and so are not shown here.) Wet climates ($MI' > 0$) are common in the Eastern United States, particularly the Northeast. A noteworthy anomaly is southern Florida, especially ecoregion sections 232G–Florida Coastal Lowlands-Atlantic, 232D–Florida Coastal Lowlands-Gulf, and 411A–Everglades. This region appears to be dry relative to other parts of the East. Although southern Florida usually receives a high level of precipitation over the course of a year, this is countered by a high level of potential evapotranspiration, which results in negative MI' values. This is categorically different from the pattern observed in the driest parts of the Western United States, especially the Southwest (e.g., sections 322A–Mojave Desert,

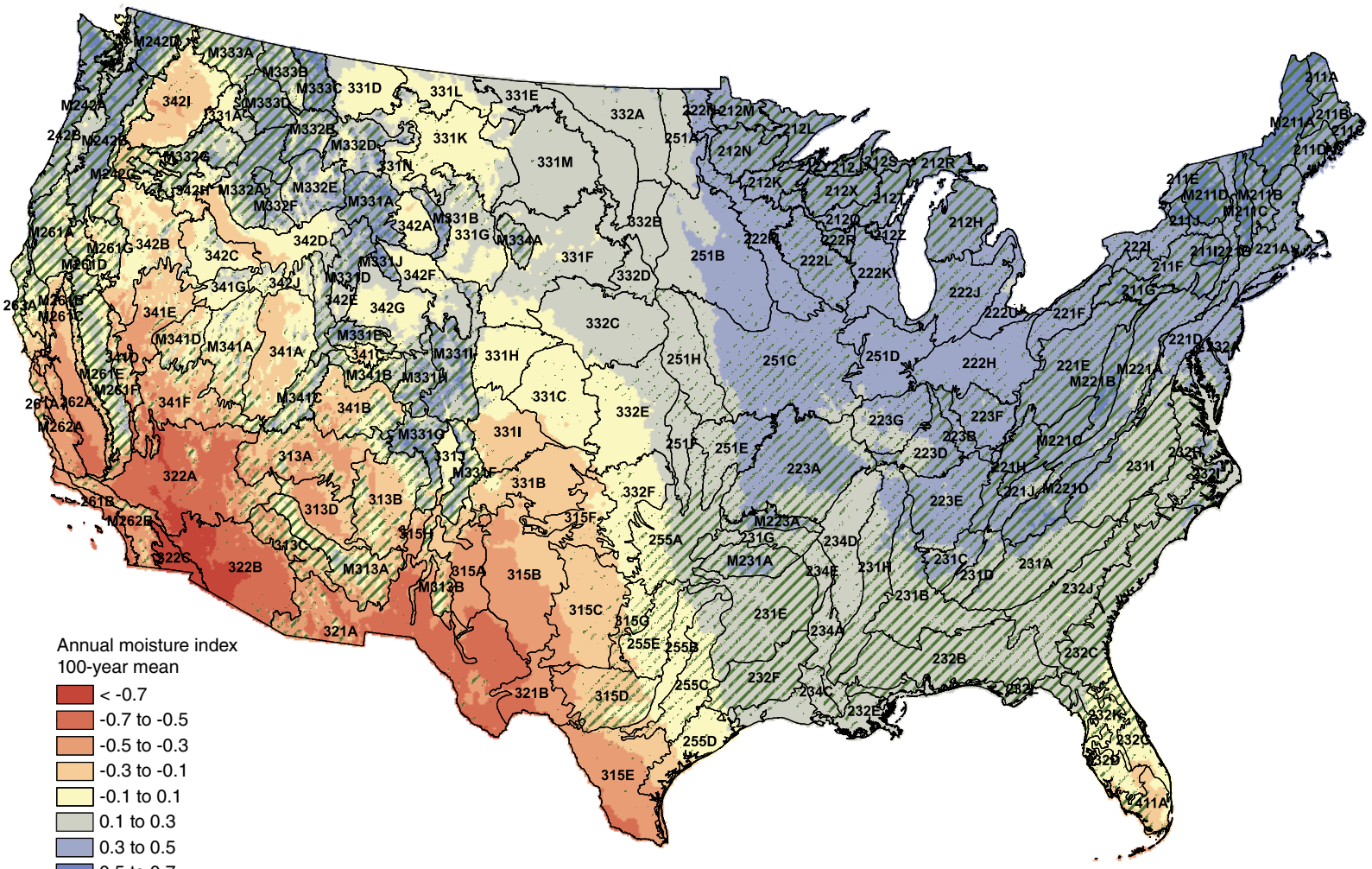

Figure 4.1—The 100-year (1915–2014) mean annual moisture index, or $MI_{1\,norm}$*, for the conterminous United States. Ecoregion section (Cleland and others 2007) boundaries and labels are included for reference. Forest cover data (overlaid green hatching) derived from Moderate Resolution Imaging Spectroradiometer (MODIS) imagery by the U.S. Department of Agriculture, Forest Service, Remote Sensing Applications Center. (Data source: PRISM Climate Group, Oregon State University)*

Table 4.1—Moisture difference *z*-score *(MDZ)* value ranges for nine wetness and drought categories, along with each category's approximate theoretical frequency of occurrence

MDZ score	Category	Frequency
		percent
< -2	Extreme drought	2.3
-2 to -1.5	Severe drought	4.4
-1.5 to -1	Moderate drought	9.2
-1 to -0.5	Mild drought	15.0
-0.5 to 0.5	Near normal conditions	38.2
0.5 to 1	Mild moisture surplus	15.0
1 to 1.5	Moderate moisture surplus	9.2
1.5 to 2	Severe moisture surplus	4.4
> 2	Extreme moisture surplus	2.3

322B–Sonoran Desert, and 322C–Colorado Desert), where potential evapotranspiration is very high, but precipitation levels are very low. In fact, dry climates ($MI' < 0$) are typical across much of the Western United States because of generally lower precipitation than the East. Nevertheless, mountainous areas in the central and northern Rocky Mountains as well as the Pacific Northwest are relatively wet, such as ecoregion sections (Cleland and others 2007) M242A–Oregon and Washington Coast Ranges, M242B–Western Cascades, M331G–South-Central Highlands, and M333C–Northern Rockies. This may be driven in part by large amounts of winter snowfall in these regions.

Figure 4.2 shows the annual (i.e., 1-year) *MDZ* map for 2014 for the conterminous United States. Much of the country saw near-normal to surplus moisture conditions during the year, but a large portion of the Southwestern United States, in a swath reaching from California to Texas, experienced moderate to extreme drought (*MDZ* < -1) conditions in 2014. Most conspicuously, a large contiguous area of extreme drought (*MDZ* < -2) covered most of northern Arizona and northwestern New Mexico. This contiguous area fell across the forested portions of several ecoregion sections: 313A–Grand Canyon, 313B–Navaho Canyonlands, 313C–Tonto Transition, 313D–Painted Desert, M313A–White Mountains-San Francisco Peaks-Mogollon Rim, 322A–Mojave Desert, and 341B–Northern Canyonlands. It also extended into the sparsely forested section 315H–Central Rio Grande Intermontane. A smaller hot spot of extreme drought occurred just to the west of this large contiguous area, primarily within sections 322A and 341F–Southeastern Great Basin. There was also a hot spot of severe to extreme drought (*MDZ* < -1.5) in central Texas, mostly in sections 255E–Texas Cross Plains and Prairie, 315D–Edwards Plateau, and 315G–Eastern Rolling Plains; only section 315D contains much forest.

Most of California experienced at least mild drought conditions (*MDZ* < -0.5) during 2014, although conditions were generally worse in the southern part of the State. For example,

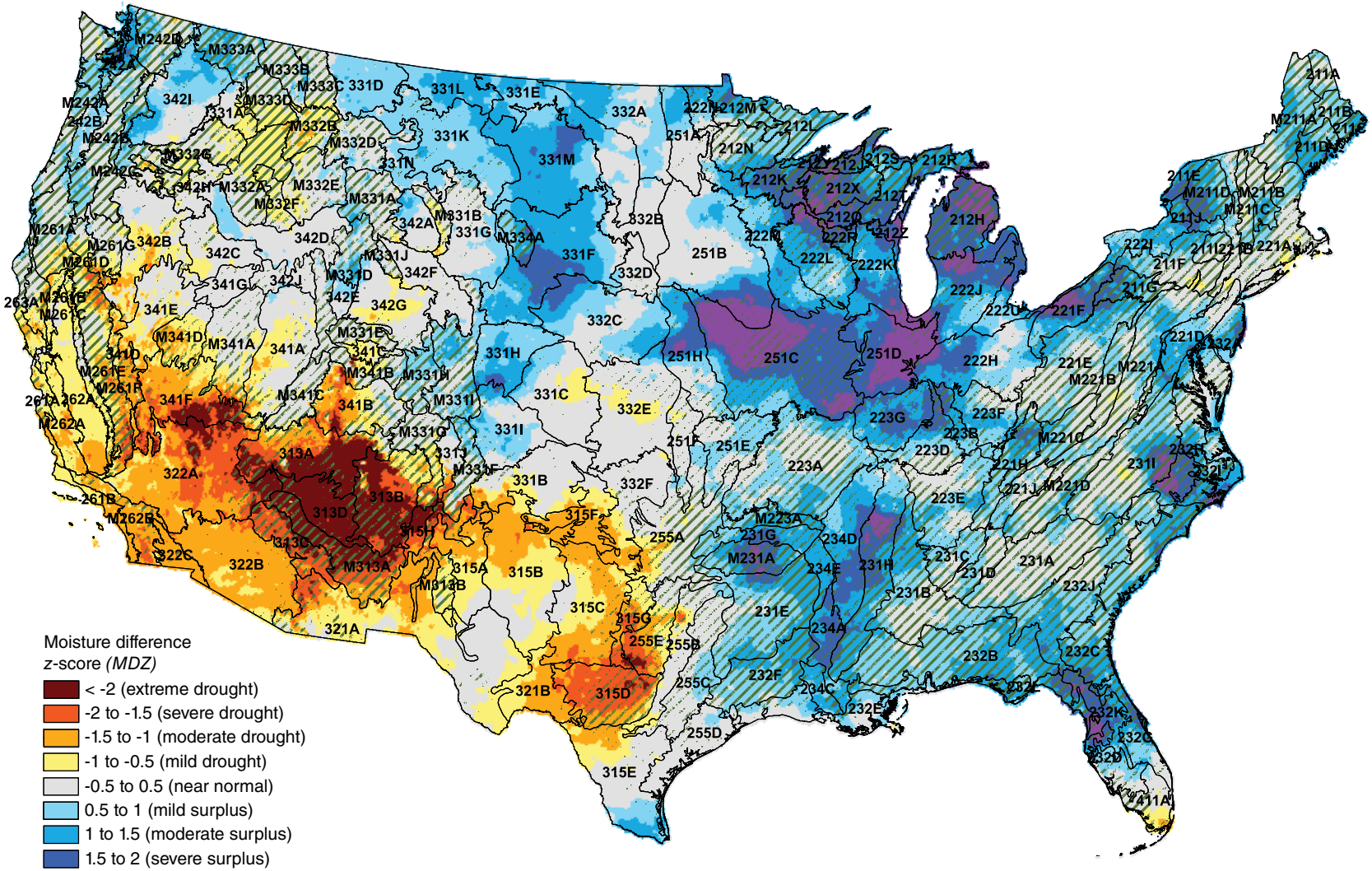

Figure 4.2—The 2014 annual (i.e., 1-year) moisture difference z*-score, or* MDZ*, for the conterminous United States. Ecoregion section (Cleland and others 2007) boundaries and labels are included for reference. Forest cover data (overlaid green hatching) derived from Moderate Resolution Imaging Spectroradiometer (MODIS) imagery by the U.S. Department of Agriculture, Forest Service, Remote Sensing Applications Center. (Data source: PRISM Climate Group, Oregon State University)*

the southern portion of section M261E–Sierra Nevada, as well as the southwestern spur of the aforementioned section 341F, contained small hot spots of severe to extreme drought conditions. In contrast, some areas within California's northernmost ecoregion sections (e.g., 263A–Northern California Coast and M261A–Klamath Mountains) actually had mild moisture surpluses during 2014. This represents a departure from the intense drought conditions that occurred almost uniformly throughout the State during the previous year, as shown in the 1-year *MDZ* map for 2013 (fig. 4.3). Indeed, 2013 was California's driest calendar year since 1895 (National Climatic Data Center 2014), as emphasized by the long list of ecoregion sections with sizeable areas of extreme drought during the year, including the aforementioned sections M261A and M261E, as well as 261A–Central California Coast, M261B–Northern California Coast Ranges, M261F–Sierra Nevada Foothills, M262B–Southern California Mountain and Valley, 263A–Northern California Coast, and 341D–Mono.

Broad-scale differences between the 2014 (fig. 4.2) and 2013 (fig. 4.3) *MDZ* maps are explained by a couple of factors. First, unusually high temperatures affected the entire Southwest in 2014 (National Climatic Data Center 2015c). Arizona, California, and Nevada had their warmest years on record; Utah had its fourth warmest year; and New Mexico had its sixth warmest year (National Climatic Data Center 2015a). For much of the region, these high temperatures increased evapotranspiration to levels that far exceeded available precipitation (National Climatic Data Center 2015c). In northern California, however, this was partially mitigated by a series of storms near the end of 2014 that pushed precipitation above normal levels. Unfortunately, these storms did not have a commensurate mitigating effect in southern California.

As is also true of the 2013 *MDZ* map, the 2014 *MDZ* map is visually striking because, outside of the Southwest, few significant drought hot spots occurred in forested parts of the United States. The only other sizeable hot spot in 2014 was an area of mild to moderate drought in the Northwestern United States, primarily in sections M332A–Idaho Batholith, M332B–Northern Rockies and Bitterroot Valley, M333D–Bitterroot Mountains, and M332F–Challis Volcanics. Overall, 2014 was, like 2013, a wet year for the country relative to historical data. The percentage of the area of the conterminous United States with moderate or worse drought conditions based on the Palmer Drought Severity Index peaked at 34.1 percent by the end of May, but decreased substantially, to 10.3 percent, by the end of December (National Climatic Data Center 2015c).

In fact, much of the Eastern United States had at least a mild moisture surplus in 2014 (see fig. 4.2). For example, the Southeast had four distinct areas with severe to extreme moisture surpluses (*MDZ* > 1.5), in North Carolina (primarily sections 232H–Middle Atlantic Coastal Plains and Flatwoods and 231I–Central Appalachian Piedmont), Florida (232D–Florida Coastal Lowlands-Gulf and 232K–Florida

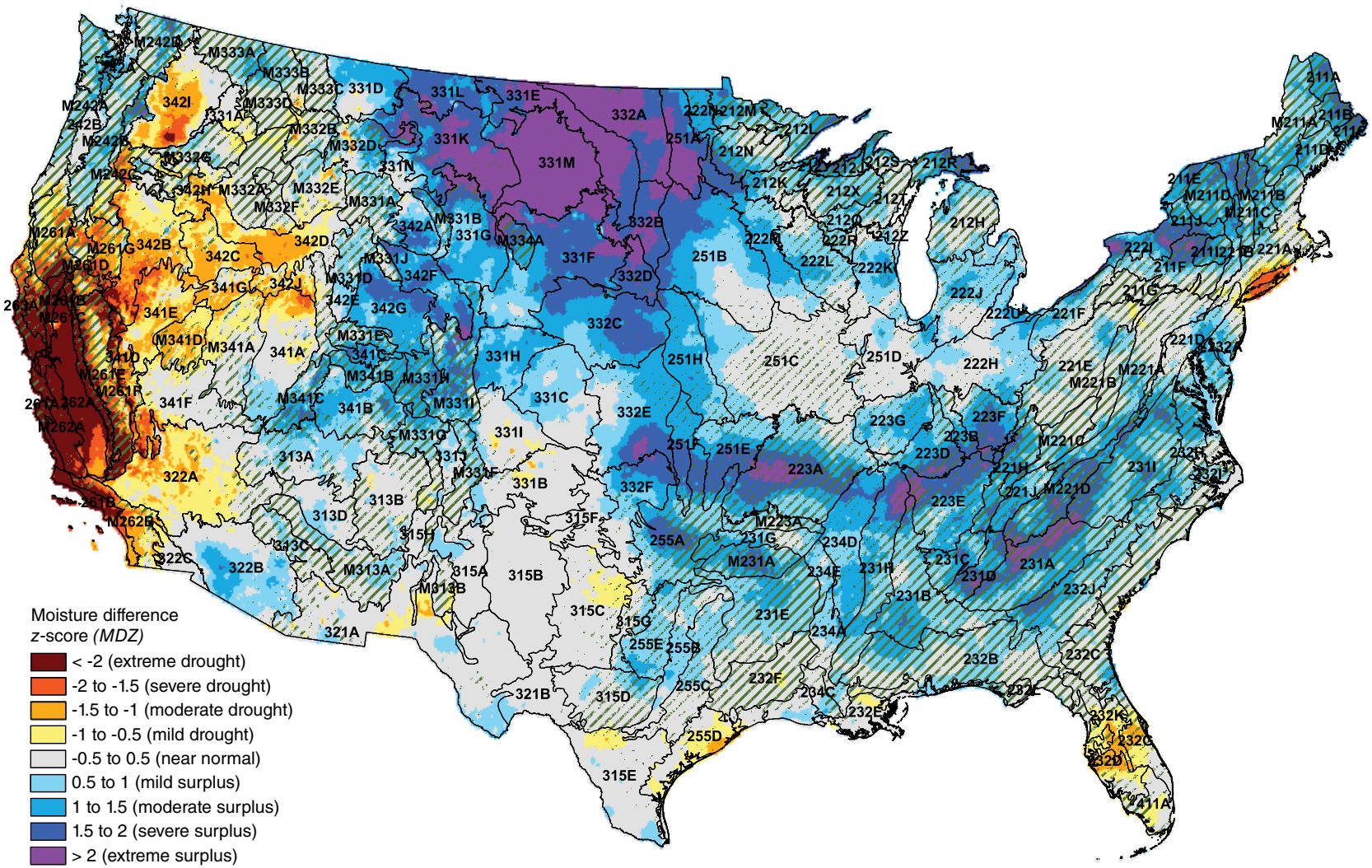

Figure 4.3—The 2013 annual (i.e., 1-year) moisture difference z-score, or MDZ, *for the conterminous United States. Ecoregion section (Cleland and others 2007) boundaries and labels are included for reference. Forest cover data (overlaid green hatching) derived from Moderate Resolution Imaging Spectroradiometer (MODIS) imagery by the U.S. Department of Agriculture, Forest Service, Remote Sensing Applications Center. (Data source: PRISM Climate Group, Oregon State University)*

Coastal Plains Central Highlands), Arkansas (231G–Arkansas Valley and M231A–Ouachita Mountains), and Tennessee (especially section 231H–Coastal Plains-Loess). Nevertheless, the most prominent areas with severe to extreme moisture surpluses during 2014 were in the Great Lakes region, including several forested sections in Ohio, Michigan, Wisconsin, and Minnesota: 212H–Northern Lower Peninsula, 212J–Southern Superior Uplands, 212K–Western Superior Uplands, 212Q–North Central Wisconsin Uplands, 212X–Northern Highlands, 212Y–Southwest Lake Superior Clay Plain, 212Z–Green Bay-Manitowac Upland, 221F–Western Glaciated Allegheny Plateau, 222L–North Central U.S. Driftless and Escarpment, and 222R–Wisconsin Central Sands. Moreover, a particularly large area of severe to extreme moisture surplus covered most of sections 251C–Central Dissected Till Plains and 251D–Central Till Plains and Grand Prairies, although neither section contains much forest. Notably, all of these areas exhibited near normal moisture conditions during 2013 (fig. 4.3). Rather, a large contiguous area of severe to extreme moisture surplus occurred further west, in the primarily nonforested Northern Great Plains region (e.g., section 331M–Missouri Plateau), while a narrow band of severe to extreme moisture surplus appeared further south (e.g., in section 223A–Ozark Highlands).

The 3-year (2012–2014; fig. 4.4) and 5-year (2010–2014; fig. 4.5) *MDZ* maps depict the recent history of moisture conditions in the conterminous United States. Perhaps most significantly, the maps clearly show that severe to extreme drought (*MDZ* < -1.5) conditions have persisted across much of the Southwestern United States for the last several years; actually, intense and widespread drought conditions have occurred in this region since the late 1990s and were also common throughout much of the 20th century (Groisman and Knight 2008, Mueller and others 2005, Woodhouse and others 2010). However, drought conditions in California and the western portion of the Southwest region appear much worse in the 3-year *MDZ* map than in the 5-year *MDZ* map, indicating that the record-setting drought conditions that have affected this region for the last few years were preceded by comparatively milder conditions in 2010 and 2011 (National Climatic Data Center 2011, 2012). A similar observation can be made for the northern portion of the Interior West region.

Elsewhere, the 5-year *MDZ* map (fig. 4.5) shows a large area of moderate to severe drought along the Gulf of Mexico coast in Texas and Louisiana, particularly in ecoregion sections 232E–Louisiana Coastal Prairies and Marshes, 232F–Coastal Plains and Flatwoods-Western

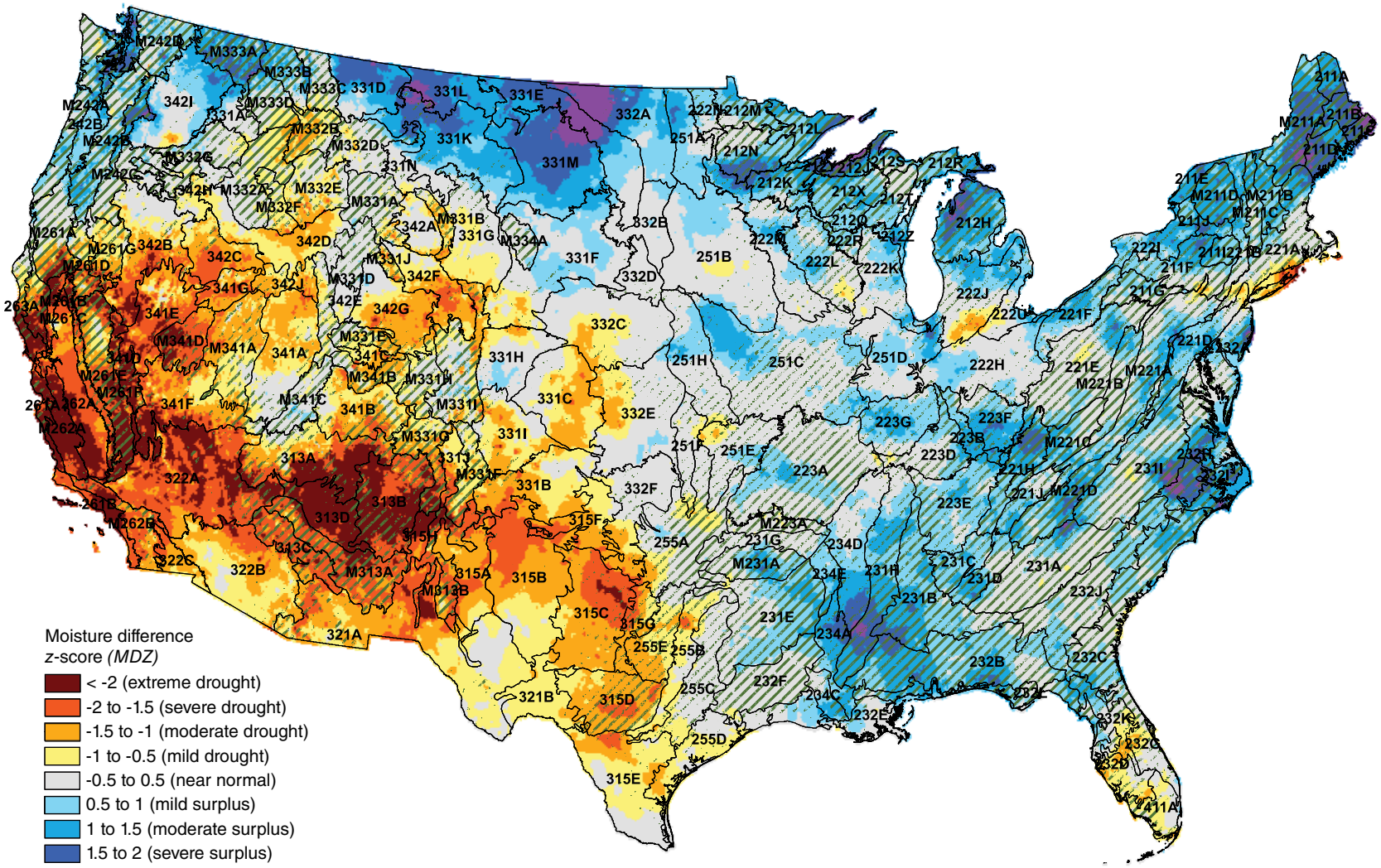

Figure 4.4—The 2012–14 (i.e., 3-year) moisture difference z*-score (*MDZ*) for the conterminous United States. Ecoregion section (Cleland and others 2007) boundaries are included for reference. Forest cover data (overlaid green hatching) derived from Moderate Resolution Imaging Spectroradiometer (MODIS) imagery by the U.S. Department of Agriculture, Forest Service, Remote Sensing Applications Center. (Data source: PRISM Climate Group, Oregon State University)*

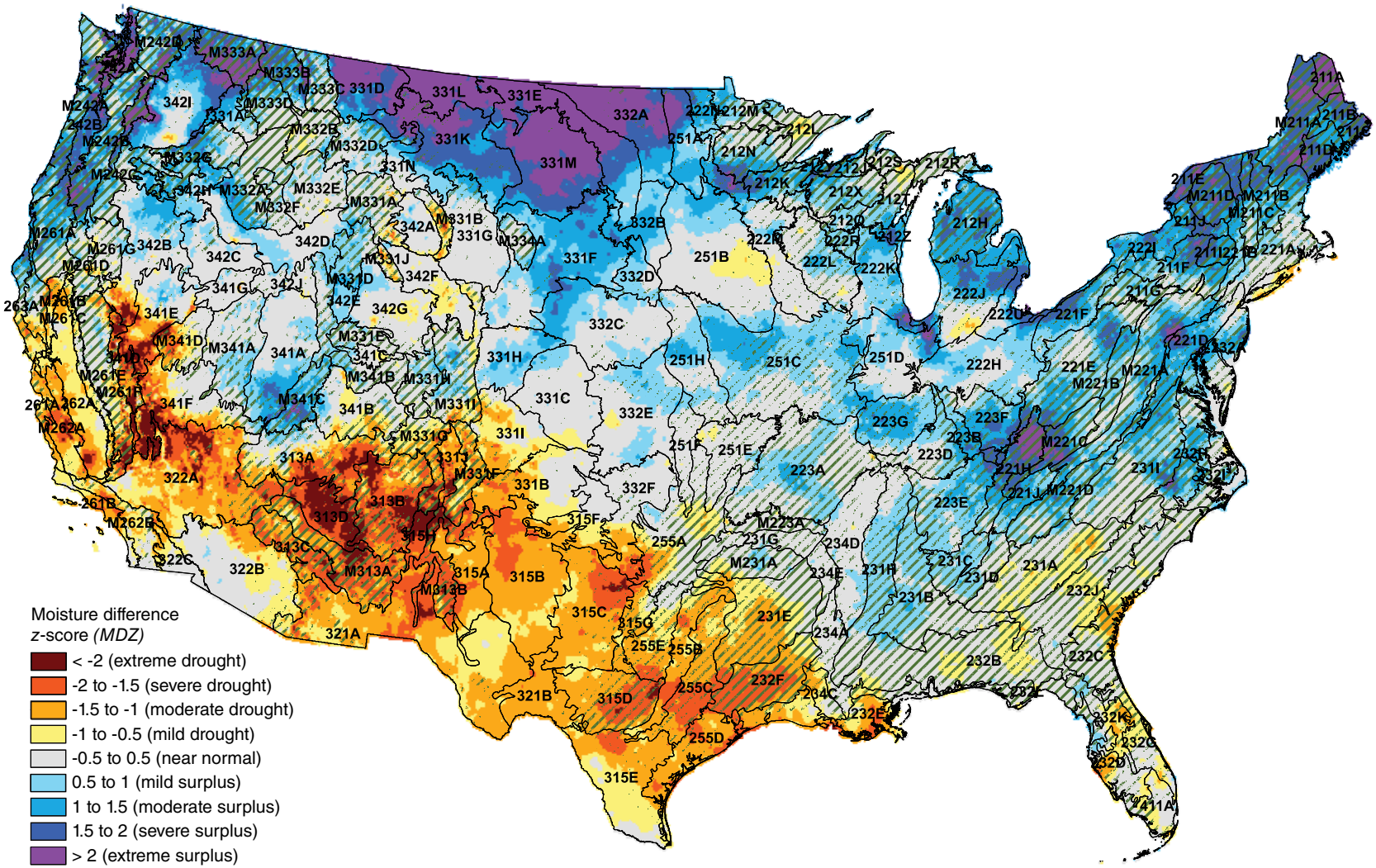

Figure 4.5—The 2010–14 (i.e., 5-year) moisture difference z*-score* (MDZ) *for the conterminous United States. Ecoregion section (Cleland and others 2007) boundaries are included for reference. Forest cover data (overlaid green hatching) derived from Moderate Resolution Imaging Spectroradiometer (MODIS) imagery by the U.S. Department of Agriculture, Forest Service, Remote Sensing Applications Center. (Data source: PRISM Climate Group, Oregon State University)*

Gulf, and 255C–Oak Woods and Prairie. By comparison, the 3-year *MDZ* map (fig. 4.4) shows little or no presence of drought conditions in these sections. Although Texas and Louisiana experienced record dryness and summer heat waves during 2010 and 2011(National Climatic Data Center 2011, 2012), the 1-year *MDZ* maps for 2013 (fig. 4.3) and 2014 (fig. 4.2) demonstrate that moisture conditions in this region have improved markedly during the last couple of years. Similarly, the 3-year and 5-year maps, as well as the 1-year map for 2013, show an area of mild to moderate drought in central Florida (sections 232D–Florida Coastal Lowlands-Gulf, 232G–Florida Coastal Lowlands-Atlantic, and 232K–Florida Coastal Plains Central Highlands) and another area of mild to severe drought in the vicinity of Long Island (in section 221A–Lower New England). However, in 2014 (see fig. 4.2) the former area displayed a moisture surplus, whereas the latter returned to near normal moisture conditions.

From a forest health perspective, the most relevant moisture surpluses are likely those that last for several years. These persistent surplus conditions are depicted in the 3-year and 5-year *MDZ* maps. For instance, the 3-year *MDZ* map (fig. 4.4) shows pockets of severe to extreme moisture surplus in various parts of the Eastern United States, including the Southeast (e.g., section 231H–Coastal Plains-Loess in Tennessee and Alabama, as well as sections 231I–Central Appalachian Piedmont and 232H–Middle Atlantic Coastal Plains and Flatwoods in North Carolina), northern New England (e.g., 211C–Fundy Coastal and Interior, 211D–Central Maine Coastal and Embayment, and M211A–White Mountains), and the Great Lakes (e.g., 212H–Northern Lower Peninsula and 212Y–Southwest Lake Superior Clay Plain). Additionally, the 3-year map shows areas of severe to extreme moisture surplus in the Pacific Northwest, primarily in sections 242A–Puget Trough, M333A–Okanogan Highland, M242C–Eastern Cascades, and M242D–Northern Cascades. The 5-year *MDZ* map (fig. 4.5) shows similar, albeit more extensive, areas of severe to extreme moisture surplus in New England and the Pacific Northwest, but there are also disparities between the maps. In particular, the moisture surplus areas in the Southeast and Great Lakes regions that are captured in the 3-year *MDZ* map do not appear in the 5-year map; instead, areas of severe to extreme surplus are shown in Kentucky (especially sections 221H–Northern Cumberland Plateau and M221C–Northern Cumberland Mountains) and Pennsylvania (sections 221D–Northern Appalachian Piedmont and M221A–Northern Ridge and Valley). This difference is explained by the high variability of moisture conditions throughout the eastern half of the country since 2010.

FUTURE EFFORTS

If the appropriate spatial data (i.e., high-resolution maps of precipitation and temperature) remain available for public use, we will continue to produce our 1-year, 3-year, and 5-year *MDZ* maps of the conterminous United States as a regular yearly component of national-scale forest health reporting. However, users should interpret and compare the *MDZ* maps presented here cautiously. Although the maps use a standardized index scale that applies regardless of the size of the time window, the window size may still merit some consideration; for instance, an extreme drought that persists over a 5-year period has substantially different forest health implications than an extreme drought over a 1-year period. Furthermore, although the 1-year, 3-year, and 5-year *MDZ* maps may together provide a comprehensive short-term overview, it may also be important to consider a particular region's longer-term moisture history when assessing the current health of its forests. For example, in geographic regions where droughts have historically occurred on a frequent (e.g., annual or nearly annual) basis, certain tree species may be better adapted to a regular lack of available moisture (McDowell and others 2008). Because of this variability in species' drought tolerance, a long period of persistent and severe drought conditions could ultimately lead to changes in regional forest composition (Mueller and others 2005); compositional changes may similarly arise from a long period of persistent moisture surplus (McEwan and others 2011). In turn, such changes are likely to affect how a region's forests respond to subsequent drought or surplus conditions. In future work, we hope to provide forest managers and other decisionmakers with better quantitative evidence regarding critical relationships between moisture extremes and significant forest health impacts such as regional-scale tree mortality (e.g., Mitchell and others 2014). We also intend to examine the role of moisture extremes as an inciting factor for other forest threats such as wildfire or pest outbreaks.

LITERATURE CITED

Adams, H.D.; Guardiola-Claramonte, M.; Barron-Gafford, G.A. [and others]. 2009. Temperature sensitivity of drought-induced tree mortality portends increased regional die-off under global-change-type drought. Proceedings of the National Academy of Sciences. 106(17): 7063–7066.

Akin, W.E. 1991. Global patterns: climate, vegetation, and soils. Norman, OK: University of Oklahoma Press. 370 p.

Allen, C.D.; Macalady, A.K.; Chenchouni, H. [and others]. 2010. A global overview of drought and heat-induced tree mortality reveals emerging climate change risks for forests. Forest Ecology and Management. 259(4): 660–684.

Alley, W.M. 1984. The Palmer Drought Severity Index: limitations and assumptions. Journal of Climate and Applied Meteorology. 23: 1100–1109.

Anderegg, L.D.L.; Anderegg, W.R.L.; Berry, J.A. 2013. Not all droughts are created equal: translating meteorological drought into woody plant mortality. Tree Physiology. 33(7): 672–683.

Archaux, F.; Wolters, V. 2006. Impact of summer drought on forest biodiversity: what do we know? Annals of Forest Science. 63: 645–652.

Clark, J.S. 1989. Effects of long-term water balances on fire regime, north-western Minnesota. Journal of Ecology. 77: 989–1004.

Cleland, D.T.; Freeouf, J. A.; Keys, J.E.; [and others]. 2007. Ecological subregions: sections and subsections for the conterminous United States. In: Sloan, A.M., tech. ed. Washington, DC: U.S. Department of Agriculture, Forest Service. Gen. Tech. Rep. WO-76D. [Map, presentation scale 1:3,500,000; colored]. Also on CD-ROM as a GIS coverage in ArcINFO format.

Clinton, B.D.; Boring, L.R.; Swank, W.T. 1993. Canopy gap characteristics and drought influences in oak forests of the Coweeta Basin. Ecology. 74(5): 1551–1558.

Daly, C.; Gibson, W.P.; Taylor, G.H. [and others]. 2002. A knowledge-based approach to the statistical mapping of climate. Climate Research. 22: 99–113.

Groisman, P.Y.; Knight, R.W. 2008. Prolonged dry episodes over the conterminous United States: new tendencies emerging during the last 40 years. Journal of Climate. 21: 1850–1862.

Grundstein, A. 2009. Evaluation of climate change over the continental United States using a moisture index. Climatic Change. 93: 103–115.

Guarín, A.; Taylor, A.H. 2005. Drought triggered tree mortality in mixed conifer forests in Yosemite National Park, California, USA. Forest Ecology and Management. 218: 229–244.

Hanson, P.J.; Weltzin, J.F. 2000. Drought disturbance from climate change: response of United States forests. The Science of the Total Environment. 262: 205–220.

Kareiva, P.M.; Kingsolver, J.G.; Huey, B.B, eds. 1993. Biotic interactions and global change. Sunderland, MA: Sinauer Associates, Inc. 559 p.

Keetch, J.J.; Byram, G.M. 1968. A drought index for forest fire control. Res. Pap. SE-38. Asheville, NC: U.S. Department of Agriculture, Forest Service, Southeastern Forest Experiment Station. 33 p.

Koch, F.H.; Coulston, J.W. 2015. Chapter 4. 1-year (2013), 3-year (2011–2013), and 5-year (2009–2013) drought maps for the conterminous United States. In: Potter, K.M.; Conkling, B.L., eds. Forest Health Monitoring: national status, trends, and analysis 2014. Gen. Tech. Rep. SRS-209. Asheville, NC: US Department of Agriculture, Forest Service, Southern Research Station: 57–71.

Koch, F.H.; Coulston, J.W.; Smith, W.D. 2012a. High-resolution mapping of drought conditions. In: Potter, K.M.; Conkling, B.L., eds. Forest Health Monitoring 2008 national technical report. Gen. Tech. Rep. SRS-158. Asheville, NC: U.S. Department of Agriculture, Forest Service, Southern Research Station: 45–62.

Koch, F.H.; Coulston, J.W.; Smith, W.D. 2012b. Mapping drought conditions using multi-year windows. In: Potter, K.M.; Conkling, B.L., eds. Forest Health Monitoring 2009 national technical report. Gen. Tech. Rep. SRS-167. Asheville, NC: U.S. Department of Agriculture, Forest Service, Southern Research Station: 163–179.

Koch, F.H.; Smith, W D.; Coulston, J.W. 2013a. Recent drought conditions in the conterminous United States. In: Potter, K.M.; Conkling, B.L., eds. Forest Health Monitoring: national status, trends, and analysis 2011. Gen. Tech. Rep. SRS-185. Asheville, NC: U.S. Department of Agriculture, Forest Service, Southern Research Station: 41–58.

Koch, F.H.; Smith, W.D.; Coulston, J.W. 2013b. An improved method for standardized mapping of drought conditions. In: Potter, K.M.; Conkling, B.L., eds. Forest Health Monitoring: national status, trends, and analysis 2010. Gen. Tech. Rep. SRS-176. Asheville, NC: U.S. Department of Agriculture, Forest Service, Southern Research Station: 67–83.

Koch, F.H.; Smith, W.D.; Coulston, J.W. 2014. Drought patterns in the conterminous United States and Hawaii. In: Potter, K.M.; Conkling, B.L., eds. Forest Health Monitoring: national status, trends, and analysis 2012. Gen. Tech. Rep. SRS-198. Asheville, NC: U.S. Department of Agriculture, Forest Service, Southern Research Station: 49–72.

Koch, F.H.; Smith, W.D.; Coulston, J.W. 2015. Drought patterns in the conterminous United States, 2012. In: Potter, K.M.; Conkling, B.L., eds. Forest Health Monitoring: national status, trends, and analysis 2013. Gen. Tech. Rep. SRS-207. Asheville, NC: US Department of Agriculture, Forest Service, Southern Research Station: 55–69.

Laurance, S.G. W.; Laurance, W.F.; Nascimento, H. E. M. [and others]. 2009. Long-term variation in Amazon forest dynamics. Journal of Vegetation Science. 20(2): 323–333.

Martínez-Vilalta, J.; Lloret, F.; Breshears, D.D. 2012. Drought-induced forest decline: causes, scope and implications. Biology Letters. 8(5): 689–691.

Mattson, W.J.; Haack, R.A. 1987. The role of drought in outbreaks of plant-eating insects. BioScience. 37(2): 110–118.

McDowell, N.; Pockman, W.T.; Allen, C.D. [and others]. 2008. Mechanisms of plant survival and mortality during drought: why do some plants survive while others succumb to drought? New Phytologist. 178: 719–739.

McEwan, R.W.; Dyer, J.M.; Pederson, N. 2011. Multiple interacting ecosystem drivers: toward an encompassing hypothesis of oak forest dynamics across eastern North America. Ecography. 34: 244–256.

McKee, T.B.; Doesken, N.J.; Kleist, J. 1993. The relationship of drought frequency and duration to time scales. In: Proceedings of the eighth conference on applied climatology. Boston, MA: American Meteorological Society: 179–184.

Millar, C.I.; Westfall, R.D.; Delany, D.L. 2007. Response of high-elevation limber pine (*Pinus flexilis*) to multiyear droughts and 20th-century warming, Sierra Nevada, California, USA. Canadian Journal of Forest Research. 37: 2508–2520.

Mitchell, P.J.; O'Grady, A.P.; Hayes, K.R.; Pinkard, E.A. 2014. Exposure of trees to drought-induced die-off is defined by a common climatic threshold across different vegetation types. Ecology and Evolution. 4(7): 1088–1101.

Monteith, J.L. 1965. Evaporation and environment. Symposia of the Society for Experimental Biology. 19: 205–234.

Mueller, R.C.; Scudder, C.M.; Porter, M.E. [and others]. 2005. Differential tree mortality in response to severe drought: evidence for long-term vegetation shifts. Journal of Ecology. 93: 1085–1093.

National Climatic Data Center. 2011. State of the climate – drought – annual report 2010. http://www.ncdc.noaa.gov/sotc/drought/201013. [Date accessed: July 28, 2015].

National Climatic Data Center. 2012. State of the climate – drought – annual report 2011. http://www.ncdc.noaa.gov/sotc/drought/201113. [Date accessed: July 28, 2015].

National Climatic Data Center. 2014. State of the climate – drought – annual report 2013. http://www.ncdc.noaa.gov/sotc/drought/201313. [Date accessed: July 19, 2015].

National Climatic Data Center. 2015a. Climatological rankings–temperature, precipitation, and drought. http://www.ncdc.noaa.gov/temp-and-precip/climatological-rankings/index.php. [Date accessed: July 28, 2015].

National Climatic Data Center. 2015b. Divisional temperature-precipitation-drought. Documentation for the nClimDiv database. ftp://ftp.ncdc.noaa.gov/pub/data/cirs/climdiv/divisional-readme.txt. [Date accessed: July 29, 2015].

National Climatic Data Center. 2015c. State of the climate – drought – annual report 2014. http://www.ncdc.noaa.gov/sotc/drought/201413. [Date accessed: July 16, 2015].

Palmer, W.C. 1965. Metereological drought. Res. Pap. No. 45. Washington, DC: U.S. Department of Commerce, Weather Bureau. 58 p.

Peng, C.; Ma, Z.; Lei, X. [and others]. 2011. A drought-induced pervasive increase in tree mortality across Canada's boreal forests. Nature Climate Change. 1(9): 467–471.

Peters, M.P.; Iverson, L.R.; Matthews, S.N. 2015. Long-term droughtiness and drought tolerance of Eastern U.S. forests over five decades. Forest Ecology and Management. 345: 56–64.

Potter, C.S.; Klooster, S.A. 1999. Dynamic global vegetation modelling for prediction of plant functional types and biogenic trace gas fluxes. Global Ecology and Biogeography. 8(6): 473–488.

PRISM Climate Group. 2015. 2.5-arcmin (4 km) gridded monthly climate data. http://www.prism.oregonstate.edu. [Date accessed: June 23, 2015].

Raffa, K.F.; Aukema, B.H.; Bentz, B.J. [and others]. 2008. Cross-scale drivers of natural disturbances prone to anthropogenic amplification: the dynamics of bark beetle eruptions. BioScience. 58(6): 501–517.

Rozas, V.; García-González, I. 2012. Too wet for oaks? Inter-tree competition and recent persistent wetness predispose oaks to rainfall-induced dieback in Atlantic rainy forest. Global and Planetary Change. 94–95: 62–71.

Rozas, V.; Sampedro, L. 2013. Soil chemical properties and dieback of *Quercus robur* in Atlantic wet forests after a weather extreme. Plant and Soil. 373(1–2): 673–685.

Schoennagel, T.; Veblen, T.T.; Romme, W.H. 2004. The interaction of fire, fuels, and climate across Rocky Mountain forests. BioScience. 54(7): 661–676.

Steinemann, A. 2003. Drought indicators and triggers: a stochastic approach to evaluation. Journal of the American Water Resources Association. 39(5): 1217–1233.

Svoboda, M.; LeComte, D.; Hayes, M. [and others]. 2002. The drought monitor. Bulletin of the American Meteorological Society. 83(8): 1181–1190.

Thornthwaite, C.W. 1948. An approach towards a rational classification of climate. Geographical Review. 38(1): 55–94.

Thornthwaite, C.W.; Mather, J.R. 1955. The water balance. Publications in Climatology. 8(1): 1–104.

Trouet, V.; Taylor, A.H.; Wahl, E.R. [and others]. 2010. Fire-climate interactions in the American West since 1400 CE. Geophysical Research Letters. 37(4): L04702.

Williams, A.P.; Allen, C.D.; Macalady, A.K. [and others]. 2013. Temperature as a potent driver of regional forest drought stress and tree mortality. Nature Climate Change. 3(3): 292–297.

Willmott, C.J.; Feddema, J.J. 1992. A more rational climatic moisture index. Professional Geographer. 44(1): 84–87.

Woodhouse, C. A.; Meko, D. M.; MacDonald, G. M. [and others]. 2010. A 1,200-year perspective of 21st century drought in southwestern North America. Proceedings of the National Academy of Sciences. 107(50): 21283–21288.